European Heart Journal (2009) **30**, 2722–2732
doi:10.1093/eurheartj/ehp265

Autologous mesenchymal stem cells produce reverse remodelling in chronic ischaemic cardiomyopathy

Karl H. Schuleri[1], Gary S. Feigenbaum[2,3], Marco Centola[1], Eric S. Weiss[4], Jeffrey M. Zimmet[1], Jennifer Turney[5], Joshua Kellner[5], Menekhem M. Zviman[1], Konstantinos E. Hatzistergos[2,3], Barbara Detrick[6], John V. Conte[4], Ian McNiece[3], Charles Steenbergen[6], Albert C. Lardo[1], and Joshua M. Hare[2,3]*

[1]Division of Cardiology, Department of Medicine, Johns Hopkins University, Baltimore, MD, USA; [2]Cardiovascular Division, Department of Medicine, Miller School of Medicine, University of Miami, Miami, FL, USA; [3]Interdisciplinary Stem Cell Institute, Miller School of Medicine, University of Miami, 1501 NW 10th Avenue, 8th Floor, Miami, FL, USA; [4]Department of Surgery, Johns Hopkins University, Baltimore, MD, USA; [5]Division of Hematology, Department of Medicine, Johns Hopkins University, Baltimore, MD, USA; and [6]Department of Pathology, Johns Hopkins University, Baltimore, MD, USA

Received 30 January 2009; revised 29 April 2009; accepted 8 June 2009; online publish-ahead-of-print 8 July 2009

Aims The ability of mesenchymal stem cells (MSCs) to heal the chronically injured heart remains controversial. Here we tested the hypothesis that autologous MSCs can be safely injected into a chronic myocardial infarct scar, reduce its size, and improve ventricular function.

Methods and results Female adult Göttingen swine ($n = 15$) underwent left anterior descending coronary artery balloon occlusion to create reproducible ischaemia–reperfusion infarctions. Bone-marrow-derived MSCs were isolated and expanded from each animal. Twelve weeks post-myocardial infarction (MI), animals were randomized to receive surgical injection of either phosphate buffered saline (placebo, $n = 6$), 20 million (low dose, $n = 3$), or 200 million (high dose, $n = 6$) autologous MSCs in the infarct and border zone. Injections were administered to the beating heart via left anterior thoracotomy. Serial cardiac magnetic resonance imaging was performed to evaluate infarct size, myocardial blood flow (MBF), and left ventricular (LV) function. There was no difference in mortality, post-injection arrhythmias, cardiac enzyme release, or systemic inflammatory markers between groups. Whereas MI size remained constant in placebo and exhibited a trend towards reduction in low dose, high-dose MSC therapy reduced infarct size from 18.2 ± 0.9 to $14.4 \pm 1.0\%$ ($P = 0.02$) of LV mass. In addition, both low and high-dose treatments increased regional contractility and MBF in both infarct and border zones. Ectopic tissue formation was not observed with MSCs.

Conclusion Together these data demonstrate that autologous MSCs can be safely delivered in an adult heart failure model, producing substantial structural and functional reverse remodelling. These findings demonstrate the safety and efficacy of autologous MSC therapy and support clinical trials of MSC therapy in patients with chronic ischaemic cardiomyopathy.

Keywords Magnetic resonance imaging • Myocardial infarction • Remodelling • Mesenchymal stem cells

Introduction

Heart failure (HF) remains a leading cause of morbidity and mortality in developed[1] and developing countries,[2] and carries a 20% 1 year mortality.[3] As such, successful cell-based therapeutic strategies for this disorder could have a substantial public health benefit.[4]

Bone-marrow-derived mesenchymal stem cells (MSCs) are easily obtainable and expandable multipotent progenitor cells,[5,6] and have emerged as attractive candidates for cellular therapies

* Corresponding author. Tel: +1 305 243 1999, Fax: +1 433 287 7945, Email: jhare@med.miami.edu

for disorders of the heart and other organ systems.[7] Experimental studies in large animals[8–11] and early clinical work[12,13] support the concept that therapeutically delivered MSCs safely improve heart function following acute myocardial infarction (MI). Whether this therapy can achieve reverse remodelling and improve left ventricular ejection fraction (LVEF) in the chronically injured heart remains unknown.

Despite the promising characteristics of MSCs as a cell therapeutic, experimental studies have raised safety concerns. For example, late passage MSCs exhibit chromosomal disorders,[14] cause tumours in rodent models,[15] and can cause ectopic bone and fat tissue formation.[16] Another recent study reported that MSCs form encapsulated structures containing calcifications after intramyocardial delivery.[17] Additional safety concerns of all cell therapies include possible transmission of infectious diseases, cell migration, potential unintended effects in non-targeted organs, immunologic reactions, and uncontrolled proliferation or neoplasia.[18]

In order to address the hypothesis that autologous MSCs safely reduce infarct size and improve cardiac function in subjects with post-MI HF, we conducted a randomized, blinded, placebo-controlled trial of bone-marrow (BM)-derived MSCs in adult mini-swine. The aims of this study were to demonstrate that (i) autologous BM-derived MSCs can be safely harvested and expanded *in vitro* from subjects with MI and left ventricular dysfunction (LVD), (ii) MSCs can be safely delivered to chronic scars in HF subjects, and (iii) MSCs reduce infarct size and improve cardiac function in chronically scarred hearts.

Methods

Induction of myocardial infarction

All animal studies were approved by the Johns Hopkins University Institutional Animal Care and Use Committee and comply with the *Guide for the Care and Use of Laboratory Animals* (NIH Publication no. 80-23, revised 1985). Female Göttingen minipigs were purchased from Marshall BioResources (North Rose, NY).

Myocardial infarction was induced by temporary balloon occlusion of the left anterior descending coronary artery (LAD) with an inflated angioplasty balloon as previously described in detail.[19] After 120 min occlusion was terminated by balloon deflation and removal, and reperfusion was established.

Bone-marrow harvest, mesenchymal stem cell isolation, and characterization

Porcine BM cells were aspirated from the iliac crest of each animal. The mononuclear cells (MNCs) were then isolated on a Ficoll gradient. The low-density fraction, which contained the MNCs, was collected and after washing placed in T162 cm^2 costar tissue culture flasks at 1–5 $\times$ 10^6 cells per mL of alpha MEM media containing 20% fetal calf serum. The cells were incubated at 5% CO_2, 37°C, and the media changed weekly. Adherent cells were identified by microscopic evaluation at Day 3 and the non-adherent cells discarded with the media with each media change. The MSC became confluent after ~2 weeks of culture and were passaged using trypsin–EDTA for cell mobilization. Cultures were expanded with each passage of the MSC until sufficient numbers of MSC were obtained. A total of four to seven passages were required.

Phenotypic characterization of the MSCs was achieved with porcine specific antibodies or human antibodies that are cross-reactive with porcine antigens. The porcine MSCs were CD45− and CD90+, consistent with human MSCs. Porcine MSCs formed CFU-F colonies similar in size, appearance, and frequency to human BM-derived MSCs. Cytogenic abnormalities were highly unlikely given the normal cell appearance and growth rate, as previously described.[20] The cells were then frozen in liquid nitrogen until needed. Prior to injection, the cells were thawed rapidly, washed to remove dimethylsulfoxide, and then re-suspended in PBS plus 1% human serum albumin to the required cell dose.

Study design

Fifteen pigs were used in this randomized, blinded, placebo-controlled pre-clinical study. Animals were allowed to recover from MI and given sufficient time for formation of a transmural MI, 111 $\pm$ 4 days (3.7 $\pm$ 0.1 months). Pigs were randomized to one of the following three groups at an age 549 $\pm$ 22 days (18.3 $\pm$ 0.7 months, *Table 1*). All animals received 15–25 needle injections, and were allocated to:

High MSC dose ($n = 6$, 200 $\times$ 10^6 MSCs),
Low MSC dose ($n = 3$, 20 $\times$ 10^6 MSCs), and
Placebo [$n = 6$, phosphate buffered saline (PBS)].

Initially, nine animals were randomized equally to the placebo, low dose, and high dose MSC groups. After an interim analysis (3 placebo, 2 low dose, 4 high dose), the six remaining animals were randomized continuing the 2:1 ratio between high and low dose and placebo. The results of these studies supported Food and Drug Administration approval for The PROMETHEUS Study (Prospective Randomized Study of Mesenchymal Stem Cell Therapy in Patients Undergoing Cardiac Surgery, clinicaltrials.gov NCT00587990, 362).

Surgical procedure

An anterior thoracotomy at the fifth intercostal space was performed. After pericardial excision, the heart was freely rotated superiorly to gain access to the apex. The apical infarction zone was visualized, and a moist gauze pack was placed on the underside of the heart to allow for exposure. The autologous BM-derived MSCs or placebo volumes were injected in 0.25 mL volumes with a 1 mL syringe equipped with a 29-gauge needle. The injections were administered epicardially into and surrounding akinetic or severely hypokinetic areas, as determined by direct visualization. A total of 15–25 injections were administered. After injections, careful haemostasis was achieved with 4-0 pledgeted prolene sutures, as necessary, and the left chest was copiously irrigated. A 20-French chest tube was inserted through a small incision just anterior to the thoracotomy and placed posteriorly in the chest. Prior to closure, intrapleural bupivicane was injected for additional peri-operative analgesia. The surgical team remained blinded to the content of the aliquots throughout the procedure and the post-operative care.

Magnetic resonance imaging

Global and regional function

Magnetic resonance images were acquired using a 1.5 T MR scanner (CV/i, GE Medical Systems, Waukesha, Wisconsin) at baseline, following MI, prior to injection and 12 weeks after cell delivery. Global and LV function was assessed using a steady-state free precession pulse sequence.[21–23] Six to eight contiguous short-axis slices were prescribed to cover the entire heart from base to apex. Image parameters were the following: TR/TE = 4.2 ms and 1.9 ms; Flip angle = 45°; 256 $\times$ 160 matrix; 8 mm slice thickness/no gap; 125 kHz; 28 cm FOV and 1 NSA.

Table 1 Baseline conditions

		Placebo	Low-dose MSC	High-dose MSC	*P*-value
Age (months)	MI	14.0 ± 0.9	14.5 ± 1.4	15.2 ± 1.3	0.74
	Injection	17.4 ± 1.0	18.4 ± 1.7	19.1 ± 1.4	0.62
	Endpoint	20.7 ± 1.1	22.0 ± 2.0	22.5 ± 1.4	0.96
Body weight (kg)	MI	31.6 ± 1.4	30.6 ± 3.3	28.5 ± 1.0	0.37
	Injection	37.8 ± 2.2	33.4 ± 2.5	33.6 ± 1.2	0.21
	Endpoint	40.8 ± 2.5	37.1 ± 0.7	36.6 ± 1.5	0.29
Follow-up (months)	After injection	3.3 ± 0.2	3.6 ± 0.3	3.4 ± 0.1	0.61

MI, myocardial infarction; MSC, mesenchymal stem cell.

To assess regional cardiac function, tagged MRI images were acquired with an ECG-gated, segmented K-space, fast gradient recalled echo pulse sequence with spatial modulation of magnetization to generate a grid tag pattern. Images were obtained at the same location as the cine-MRI images, and image parameters were as follows: TR/TE = 6.7 and 3.2 ms; flip angle = 12°; 250 × 160 matrix; views per second: 4; 8 mm thickness/no gap; 31.25 kHz; 28 cm FOV; 1 NSA and six pixels tagging space.

Myocardial perfusion imaging and delayed enhancement

First-pass perfusion imaging was performed continuously for ~1.5 min at rest immediately after an intravenous bolus injection of Gd-DTPA (0.1 mmol/kg, 5 mL/s; Magnevist, Berlex, Wayne, NJ) with an ECG-gated interleaved saturation recovery gradient echo planar imaging pulse sequence (EFGRET-ET). An entire short-axis stack was acquired every 2–4 heartbeats. Imaging parameters were as follows: TR/TE = 7.2 and 1.8 ms; flip angle = 20°; 128 × 128 matrix; 8 mm slice thickness/no gap; bandwidth 125 kHz; 28-com FOV; and 0.5–1 NSA.

After completion of first-pass image acquisition a second bolus of Gd-DTPA (0.1 mmol/kg) was injected. Prior to the second bolus of Gd-DTPA, infusion of adenosine was used to simulate a stress response. Delayed enhancement (DE) images were acquired 15 min later with an ECG-gated, breath-hold, interleaved, inversion recovery, fast gradient echo pulse sequence. DE-MRI images were acquired at the same location as the short-axis cine images. Imaging parameters were TR/TE/inversion time (TI) = 7.3, 3.3, and ~200 ms; flip angle = 25°; 256 × 196 matrix; 8 mm slice thickness/no gap; 31.2 kHz; 28 cm FOV; and 2 NSA. Inversion recovery time was adjusted as need to null the normal myocardium.[9]

Magnetic resonance imaging analysis

Cine and DE MR images were analysed for determination of global function, infarct quantization, and remodelling parameters using a custom research software package (Segment; http://segment.heiberg.se) as previously described.[24] Tagged and perfusion MRI images were analysed using a commercially available software package (PLUS, Diagnosoft Inc., Baltimore, MD). The four most apical tagged slices were selected and overlaid with the corresponding DE slices. Meshes were constructed with a total of 72 evenly distributed regions (24 endocardial, 24 mid-wall, and 24 epicardial) incorporating the entire myocardium. The meshes were designed such that the edges of the infarct scar corresponded with the edges of mesh regions. The border zone was defined as the left and right most infarct containing mesh regions, and the infarct zone encompassed all regions in between. The same slices, mesh, and defined regions were used at all time points on an individual pig basis. The values calculated were averaged between all like defined regions and across all slices.

Laboratory measurements and cytokine analysis

Blood chemistry and white blood counts were obtained through a clinical laboratory immediately following each blood draw. Blood for cytokine analysis was also collected at this time, centrifuged at 2000*g* for 15 min at 4°C, serum recovered, aliquoted, and stored in a −70 freezer until analysed. Porcine-specific serum levels of TGF-beta and TNF-alpha were determined using commercially available enzyme-linked immunosorbent assay (EIA) kits (R&D Systems, Minneapolis, MN). Serum samples were tested in duplicate according to the manufacturer's instructions. The mean minimum detectable dose for each cytokine measured is TGF-β = 4.6 pg/mL and TNF-α = 3.7 pg/mL.

Statistics

All measurements are expressed as mean ± standard error. The Mann–Whitney test and *t*-tests were performed, as appropriate, to test for significance between variables using commercially available software (Stata, StataCorp LP, College Station, TX). $P < 0.05$ was defined as statistically significant. The Kruskal–Wallis test was used to compare age, bodyweight, and follow-up time (*Table 1*). The impact of cell therapy on TGFb levels were evaluated using repeated measures ANOVA. Comparisons between placebo and the two cell dose groups used two-way ANOVA. *Post hoc* analysis was performed with the Mann–Whitney test.

Results

Safety and tolerability

Baseline conditions and laboratory values

Baseline conditions for the animals are shown in *Table 1*. As depicted, animals in the three groups had similar age and weight throughout the course of the study, and were followed for similar periods of time.

Plasma levels of cardiac enzymes and white blood cell count were comparable between the groups studied (*Figure 1*). In addition to standard laboratory values, we also measured two cytokines, TGF-β and TNF-α. Prior to cellular transplantation (Day 1A), TGF-β levels were ~13 500 pg/mL. In the high-dose MSC group, this level fell 24 h later to 9000 pg/mL ($P < 0.05$), and interestingly

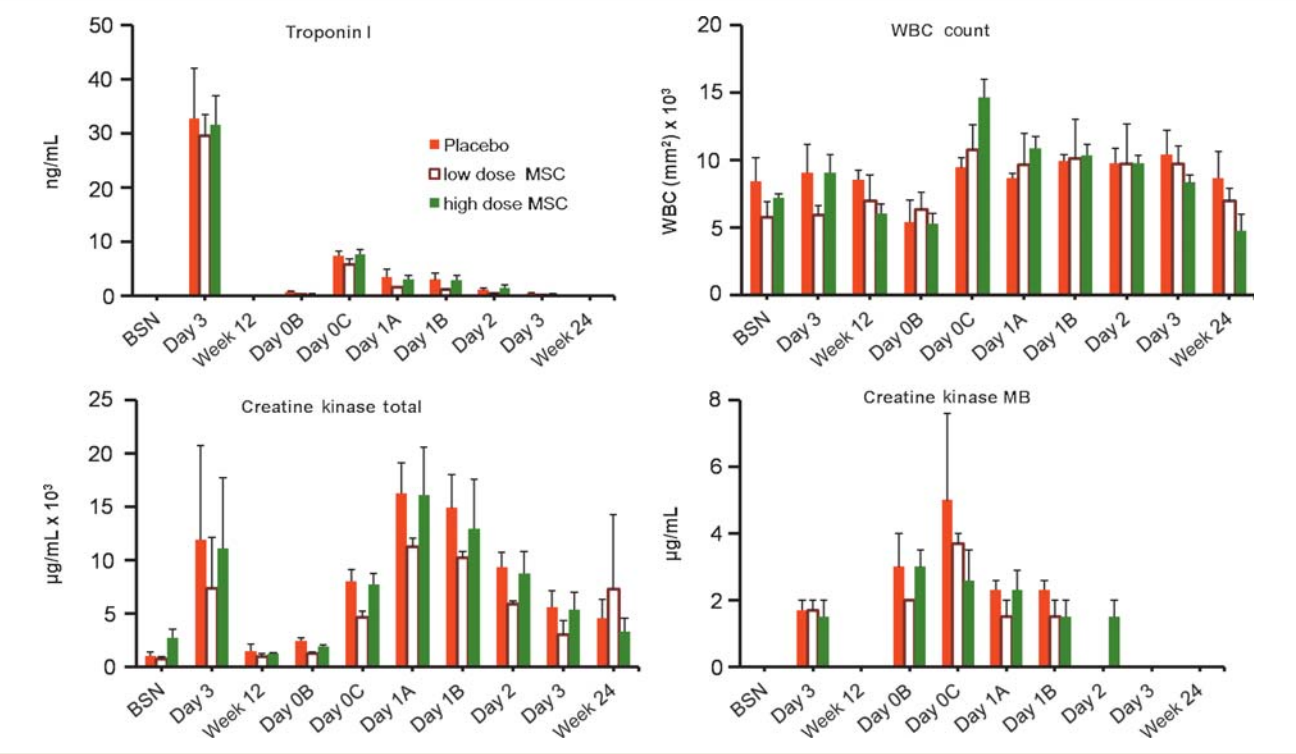

Figure 1 Blood and serum markers of inflammation and myocardial tissue damage. There is no significant difference between placebo, low-dose, and high-dose-treated animals immediately post-myocardial infarction and 12 weeks after injection.

rose over 3 days back to baseline levels ($P < 0.001$ repeated measures ANOVA). This decrement was smaller in the low dose MSC group and absent in the placebo animals ($P < 0.03$ for high dose vs. placebo, *Figure 2*). In contrast, levels of TNF-α were similar following surgical cellular transplantation and 12 weeks after surgery (data not shown), and were not affected by MSC injection.

Histology

Histology was examined by an experienced cardiac pathologist (C.S.) blinded to animal treatment group. Transmural infarcts were observed in all hearts. The infarcts were characterized by densely collagenized scar tissue with mild-to-moderate cellularity, due mostly to fibroblasts, and mild-to-moderate vascularity. There were rare, very small foci of inflammation composed of lymphocytes and macrophages, with minor myocyte damage and necrosis (*Table 2* and *Figure 3*). Many of the hearts had a mild degree of pericardial fibrosis, attributable to the surgical procedure. Rarely, small foci of mature fat and calcification within the scar were also observed, consistent with known histology of healed MI. Teratomas or other neoplastic processes were not identified in any of the hearts. Clusters of MNCs resembling stem cells were not identified in any of the hearts. Overall, there were no major differences between placebo, low dose, and high dose MSC treated animals.

Programmed stimulation and arrhythmia monitoring

All animals were monitored for cardiac arrhythmias after injection of the MSCs using implantable continuous monitoring. Although one pig exhibited transient heart block after surgery, ventricular arrhythmias or sudden deaths did not occur throughout the study period. In addition, arrhythmias were not induced during electrophysiologic programmed stimulation (placebo, $n = 3$, low dose, $n = 3$, high dose, $n = 5$) performed 12 weeks after injection and prior to sacrifice.

Efficacy

Infarct size

Infarct size and dimensions were determined using DE MRI images. There was no difference in infarct size or morphology between the three groups 12 weeks after MI (*Table 3*). We next determined the impact of cell therapy upon infarct size, measured as a percentage of the LV and as absolute volume of scar tissue. There was a trend towards a decrease in scar size in low dose and a 1.7 ± 0.4 mL decrease in scar volume in high dose ($P = 0.03$ week 12 vs. week 24) groups when compared with no-change in the placebo group (*Table 3* and *Figure 4*).

The decrease in scar size also manifested as a decrease in the circumferential extent of the infarct scar, consistent with reverse remodelling. While the infarct region showed a trend for expansion in the placebo group, it was reduced by $18.8 \pm 3.5\%$ in low dose ($P = 0.002$ vs. placebo) and $30.5 \pm 3.2\%$ ($P < 0.001$ vs. placebo and 12 week time-point) in high dose (*Table 3*). This effect was mirrored in the infarct region wall thickness, where there was continued thinning ($-9.1 \pm 6.6\%$ decrease) in the placebo group while both low and high dose groups had significant thickening (*Table 3*).

Contractility

In order to determine the regional contractile capacity of the new tissue that replaced the scar, tagged MRI images were obtained and used to calculate peak Eulerian circumferential shortening (Ecc). By defining and differentiating between the infarct, border, and remote zones the treatment could be further tracked. As shown (*Figure 5*) at the 12 week time point all animals had decreased function in the infarct $-3.1 \pm 0.4\%$ and border $-6.0 \pm 0.4\%$ zones. The depression in function in both regions continued over the course of the follow-up period in the placebo-treated animals.

In contrast contractile function in both low- and high-dose-treated animals showed significant improvement over the follow-up period. This effect was particularly evident in the border zone where peak negative Ecc decreased in low dose $-2.7 \pm 1.2\%$ ($P = 0.20$ week 12 vs. week 24, $P = 0.03$ vs. placebo) and high dose $-4.0 \pm 0.8\%$ ($P = 0.002$ week 12 vs. week 24, $P = 0.004$ vs. placebo) groups. Surprisingly, the high-dose-treated animals also showed contractile improvement in the infarct region with a decrease in peak Ecc of $-3.2 \pm 0.3\%$ ($P = 0.003$ week 12 vs. week 24, $P < 0.001$ vs. placebo) (*Figure 5*).

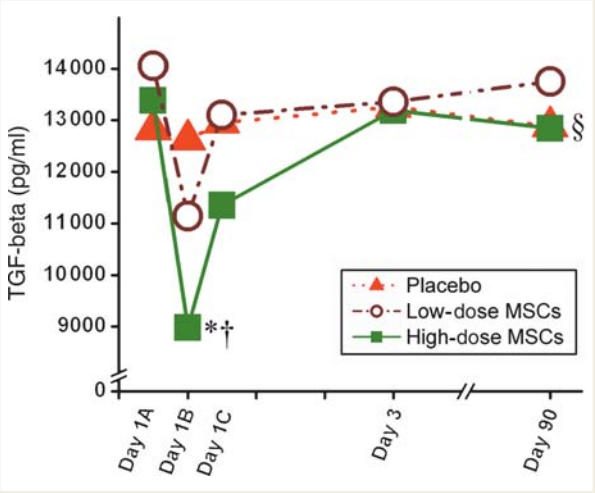

Figure 2 TGF-β serum levels after surgery. Within 24 h of stem-cell transplant, there is a dramatic drop (Day 1B) in the circulating levels of TGF-β in the high-dose mesenchymal stem cell group (*$P < 0.05$ vs. placebo, †$P < 0.05$ Day 1A vs. Day 1B), which recovers by Day 3. The low-dose mesenchymal stem cell animals follow the same pattern, but to a smaller extent. Ninety days after surgery the serum levels of TGF-β are not significantly different. (§$P < 0.001$ high-dose mesenchymal stem cell group repeated measures ANOVA).

Perfusion

First-pass perfusion MRI was used to assess whether newly formed tissue had adequate MBF. The average upslope of gadolinium to peak normalized to the LV blood was used as a measure of tissue perfusion. At the pre-injection time point all animals had diminished flow in infarct 0.12 ± 0.01 and border 0.16 ± 0.01 zones (when compared with the remote zone). In addition, coronary flow reserve determined by adenosine stimulation revealed marked attenuation. Twelve weeks after myocardial injection, the decrease basal flow and CFR persisted in placebo-treated animals. In contrast, both basal flow and CFR increased in low- and high-dose groups (*Figure 6*).

Table 2 Summary of histo-pathological findings

	Placebo ($n = 4$)				High-dose MSC ($n = 6$)				Low-dose MSC ($n = 6$)			
	Absent	Mild	Moderate	Severe	Absent	Mild	Moderate	Severe	Absent	Mild	Moderate	Severe
Cells within infarct		3[a]	1[b]			5[a]	1[a]			3		
Vascularity of infarct		4				5	1			3		
Myocarditis	4				6				2	1		
Fibrosis away from infarct	2	2			5	1			2	1		
Necrosis away from infarct	4				6				2	1[c]		
Granulation tissue outside infarct	4				6				3			
Endocardial thickening		3	1		3	2	1		2		1	
Pericardial thickening		2	2		1	3	2				2	1
Pericarditis	4				5	1			3			
Teratoma	4				6				3			
Calcification within infarct	4				5	1[c]			3			

MSC, mesenchymal stem cell.
[a]Mostly fibroblasts.
[b]Mostly cardiac myocytes.
[c]Rare foci.

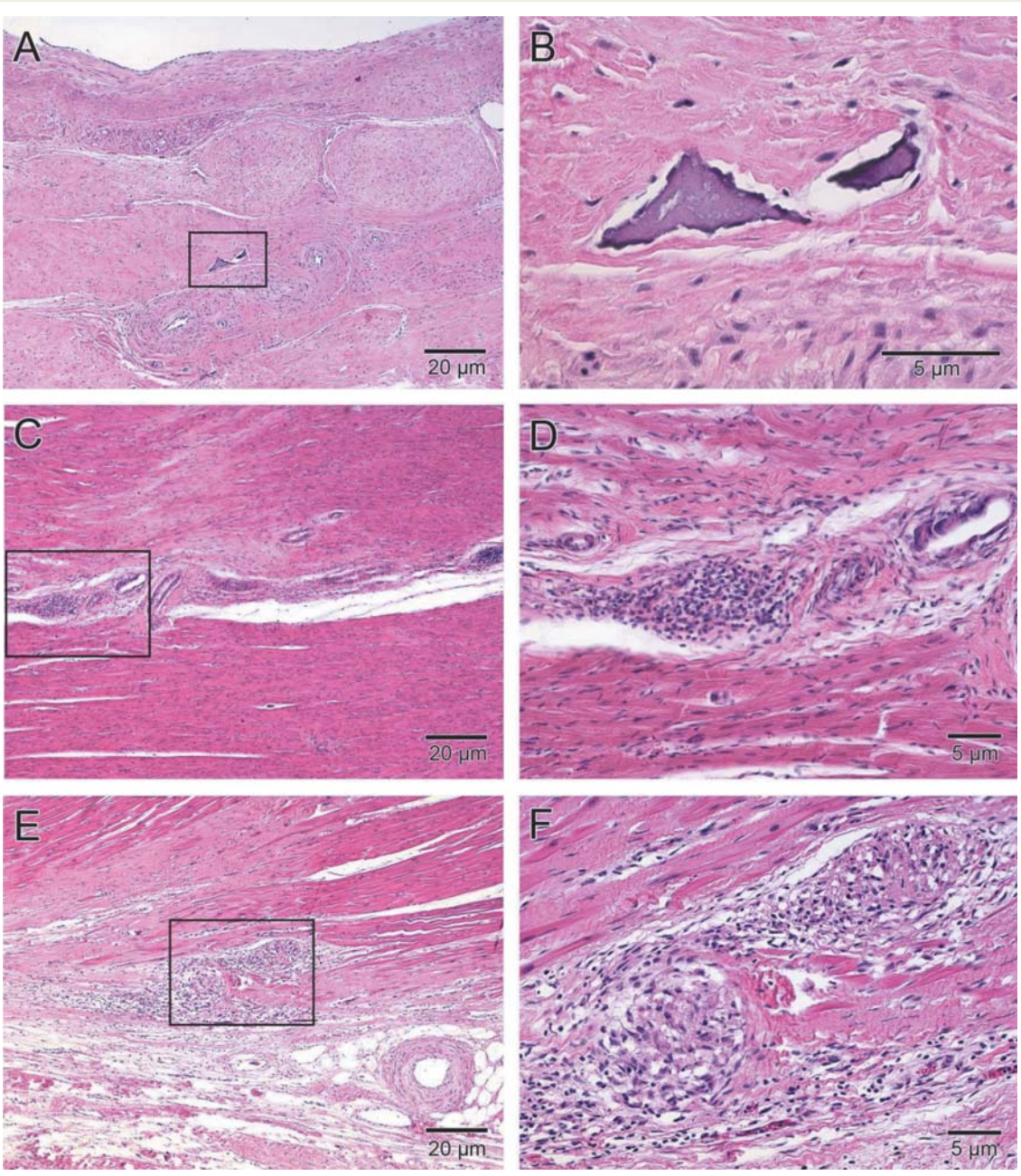

Figure 3 Isolated dystrophic cardiac calcinosis in a chronic infarct scar. (*A* and *B*) An isolated focus of calcification in dense scar tissue from a porcine heart injected with 200 × 10^6 autologous mesenchymal stem cells surrounded by dense collagen fibres and mainly fibroblasts. (*C*–*F*) Example of localized inflammation 12 weeks after injection of 200 × 10^6 MSCs. (*C* and *D*) Inflammatory cells not particularly organized and located near a large vessel in the viable myocardium. The only example of a large focus of inflammation is shown in (*E*) and (*F*). Two focal islands of inflammatory cell infiltrates in the centre scar region and at the border region of the infarct. The higher magnification of the dense collection of lymphocytes and macrophages demonstrates interspersed angiogenesis in (*F*). All samples were stained with haematoxylin and eosin.

Global left-ventricular function

The decrease in infarct size together with increased contractility and perfusion resulted in improved global LV function. Whereas EF remained constant in placebo, it increased in the high-dose-group (*Figure 7*).

Discussion

To date most attention in cardiac cell therapy has focused on treating acute MI. Here we addressed the hypothesis that autologous MSCs have substantial benefit on structure and function of the

Table 3 Infarct parameters before and 12 weeks after surgery

		Week 12	Week 24	*P*-value
MI size (% of LV mass)	Placebo	17.3 ± 1.6	18.5 ± 1.2	0.57
	Low-dose MSC	16.3 ± 1.1	12.5 ± 1.0	0.06*
	High-dose MSC	18.2 ± 0.9	14.4 ± 1.0	0.018*†
Infarct volume (cc)	Placebo	8.0 ± 0.9	8.8 ± 1.1	0.59
	Low-dose MSC	7.3 ± 0.5	6.0 ± 1.2	0.37
	High-dose MSC	8.2 ± 0.4	6.6 ± 0.5	0.03†
LV mass (g)	Placebo	45.9 ± 1.4	47.2 ± 3.6	0.75
	Low-dose MSC	45.1 ± 2.1	47.2 ± 4.9	0.71
	High-dose MSC	45.3 ± 0.7	46.1 ± 1.2	0.58
Circumferential extent (% LV circumference)	Placebo	43.8 ± 1.4	45.3 ± 0.8	0.39
	Low-dose MSC	44.7 ± 2.3	36.4 ± 3.3	0.11*
	High-dose MSC	44.3 ± 2.1	31.4 ± 1.3	0.001*†
Infarct thickness (mm)	Placebo	4.0 ± 0.1	3.6 ± 0.2	0.12
	Low-dose MSC	3.3 ± 0.1	4.9 ± 0.5	0.035*†
	High-dose MSC	3.9 ± 0.2	4.9 ± 0.4	0.049*†
Remote thickness (mm)	Placebo	7.1 ± 0.5	7.4 ± 0.5	0.69
	Low-dose MSC	6.9 ± 0.5	7.6 ± 0.5	0.38
	High-dose MSC	6.6 ± 0.5	6.9 ± 0.3	0.62

All values were calculated based on delayed contrast enhanced magnetic resonance imaging.
MI, myocardial infarction; LV, left ventricular.
*$P < 0.05$ vs. placebo.
†$P < 0.05$ week 12 vs. week 24.

LV in adult mini-swine with healed MI scars. The major findings of this study are that autologous MSCs can be safely and effectively prepared post-MI and delivered surgically in a porcine model of ischaemic HF. In addition, this therapy produced an extraordinary magnitude of benefit including reduced infarct size, new tissue that is contractile and perfused, and overall increase in LVEF. These findings provide important pre-clinical data supporting the clinical development of this approach.

Our data are in agreement with a growing number of studies performed in relevant large animal models indicating that BM-derived MSCs exert clinically meaningful cardiac repair.[8–11,25] While the mechanisms underlying this effect are controversial and likely multi-factorial, it is clear that this therapeutic approach contains merit and therefore should be pursued. The cell-therapy caused unambiguous reverse remodelling by reducing the circumferential extent of the infarct scar and increasing LVEF following a single administration of MSCs. These data support the ongoing conduct of the Prospective Randomized Study of Mesenchymal Stem Cell Therapy in Patients Undergoing Cardiac Surgery (PROMETHEUS).

Safety issues

Cell therapy for heart diseases is at an early stage and requires thorough evaluation of both short- and long-term complications of the therapy. A leading concern arises from findings in cultured MSCs that structural and chromosomal abnormalities can occur at late passage.[16] These findings are more prevalent in rodent cells where prolonged expansion, post senescence MSC cultures displayed chromosomal abnormalities, as well as an altered phenotype and changes in morphology.[15] Of great concern, these cells are described to produce tumours when injected into immunocompromised mice. In contrast, genetic stability is demonstrated in MSCs derived from human adipose tissue even when maintained in long-term culture.[14] In addition to tumour formation, BM cells and MSCs can form ectopic tissue including bone, heterotopic ossification, and fat tumours after intramyocardial injection.[17] We did not observe severe ectopic or heterotropic calcification or bone formation in our porcine model. The sparse focal calcifications we observed can be attributed to cell necrosis and/or calcification of extracellular matrix proteins, as is reported in humans with healed MI.[26] While our observations are consistent with an expected response to MI, we cannot exclude a contribution of the MSCs to the microcalcifications. The lack of osteoblasts in the vicinity of the calcification suggests that the mechanism of calcification is unrelated to active bone synthesis by autologous MSCs. This observation is in concordance with recently published data in a rat model demonstrating the presence of dystrophic cardiac calcinosis in scar tissue, which is as a tightly regulated process involving non-collagenous matrix proteins.[27]

A final major safety issue is the development of ventricular arrhythmias, which has been reported after skeletal myoblasts have been injected into non-viable myocardium.[28,29] We performed arrhythmia monitoring and programmed stimulation in our study and detected no evidence of pro-arrhythmia.

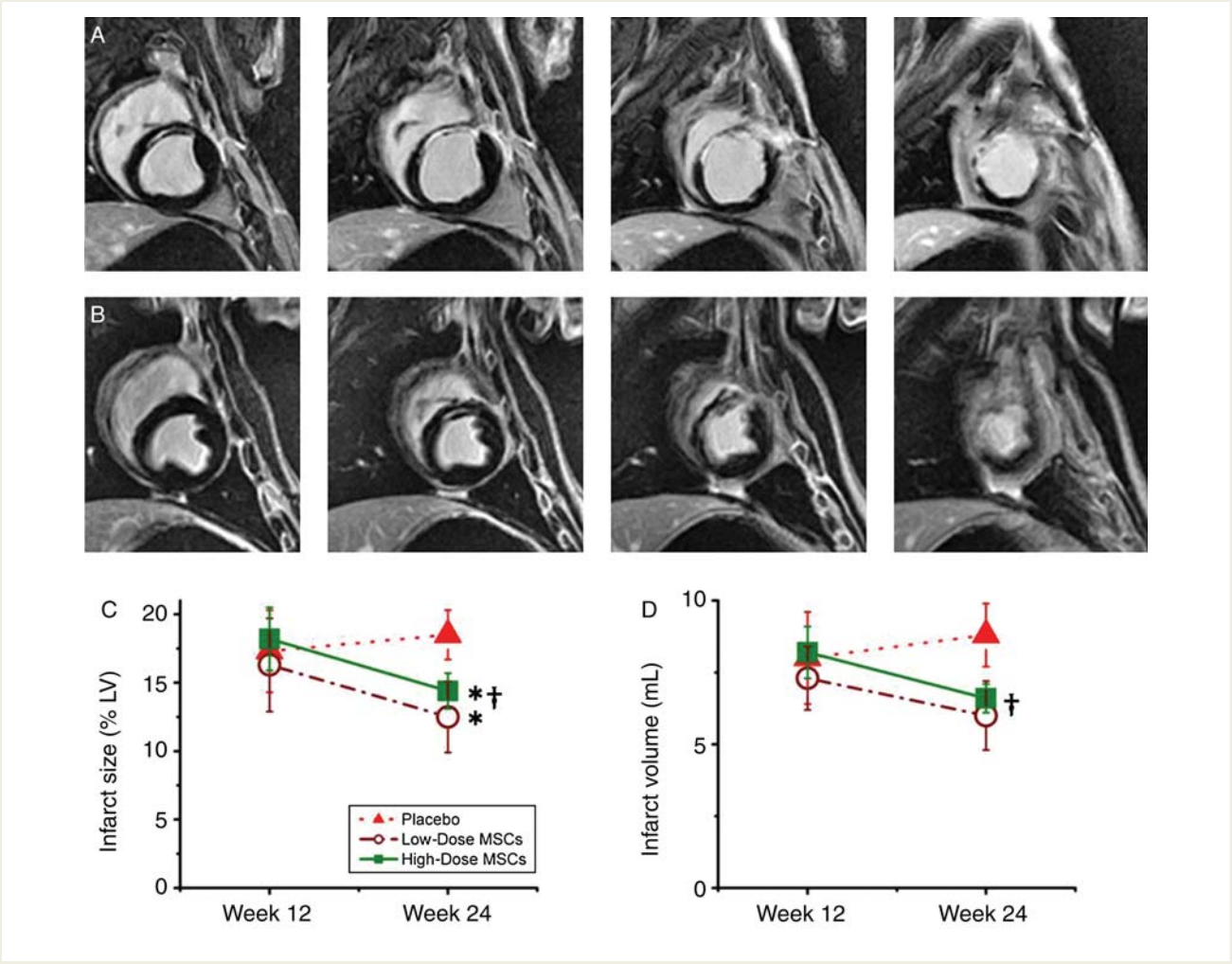

Figure 4 Impact of autologous mesenchymal stem cells therapy on chronic infarct scar remodelling in heart failure. (*A*) Contiguous short-axis delayed enhanced magnetic resonance imaging images show an example of an untreated animal 12 weeks after injection. The thinned infarct scar and the dilated ventricle can be appreciated. (*B*) Corresponding images from a high-dose-treated animal. The scar region is thicker and viable myocardium can be appreciated surrounding the scar tissue. (*C* and *D*) The effect of mesenchymal stem cell treatment on scar percentage of left ventricular and absolute volume of scar tissue (*$P < 0.05$ vs. placebo, †$P < 0.05$ week 12 vs. week 24).

Mechanism for mesenchymal stem-cell-induced cardiac repair

There are several general mechanisms invoked as explanations for the impact of cell therapy, including cell differentiation, paracrine effects, fusion, and simulation of endogenous repair.[30–34] In terms of paracrine effects, MSCs secrete cytokines that stimulate vasculogenesis and angiogenesis[32,33] as well as anti-fibrotic effects through regulation of cardiac fibroblasts proliferation and transcriptional down regulation of types I and III collagen syntheses.[35] These features of MSC may be beneficial for the treatment of HF in which fibrotic changes are involved.[25,35] Although we did not measure long-term cytokine release long term, we did observe both an improvement in tissue perfusion as well as a reduction in scar size with MSC therapy, suggesting that both of these mechanisms were operative.

We did observe a reduction in TGF-β levels in animals treated with a high dose of MSCs. A number of studies have identified a critical role for TGF-β in the induction of cardiac differentiation in embryonic stem cells.[36–38] A recent study demonstrated that treatment of MSCs with isolated proteins from infarct tissue augmented expression of cardiac specific genes. This expression profile was blocked by inhibition of TGF-β. Additional cell and electro-physiologic *in vitro* experiments showed that these differentiated MSCs expressed cardiomyocyte-specific markers, and were able to couple with cardiomyocytes.[39] In this report, we show that high levels of TGF-β are detected in the sera of normal pigs with HF. Within 30 min of MSC transplantation, there is a dramatic and significant drop in the circulating levels of TGF-β in a dose-dependent manner. It is interesting to speculate that the transplanted stem cells bind the circulating TGF-β,[40] more cells binding more TGF-β, and use this signalling pathway to trigger

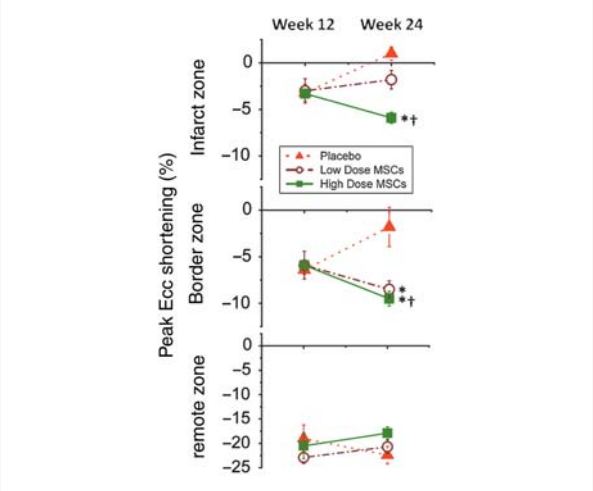

Figure 5 Plots of peak circumferential shortening (peak Ecc) in the infarct, border, and remote zones. Peak negative Ecc values represent myocardial shortening and increased contractility, whereas increasingly positive values indicate myocardial dysfunction. Ecc improves after cell therapy in both low- and high-dose cell groups in infarct border zones. In contrast, Ecc improves in infarct zones only in the high and not the low-dose MSC group. (*$P < 0.05$ vs. placebo, †$P < 0.05$ week 12 vs. week 24).

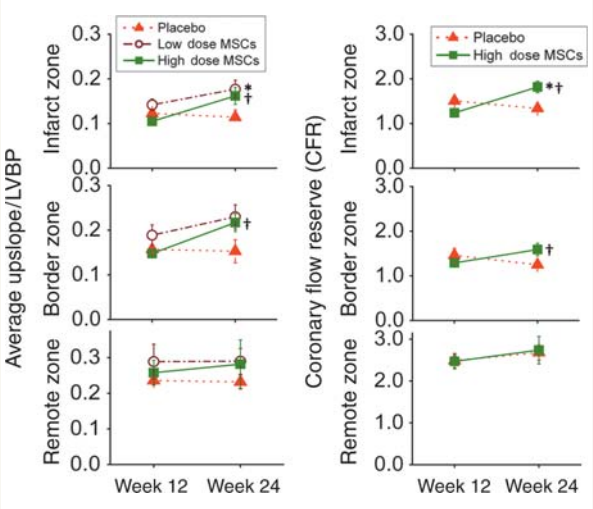

Figure 6 Plot of the average upslope to peak myocardial blood flow, normalized by left-ventricular blood pool intensity, in the resting state and the coronary flow reserve (stressed myocardial blood flow divided by resting myocardial blood flow), in the infarct, border, and remote zones. A higher value is indicative of greater flow. (*$P < 0.05$ vs. placebo, †$P < 0.05$ week 12 vs. week 24).

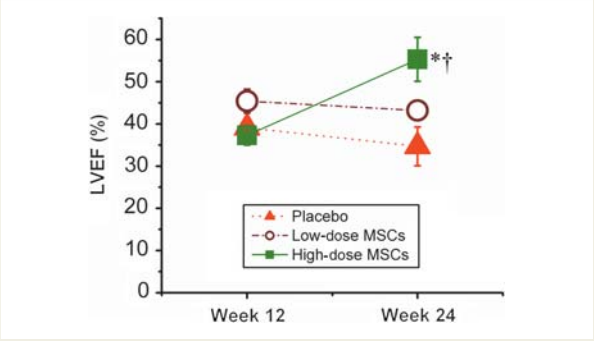

Figure 7 Impact of autologous mesenchymal stem cells therapy on global ventricular function in animals with ischaemic cardiomyopathy assessed by magnetic resonance imaging. Ejection fraction is reduced in all groups 12 weeks post-MI and remains depressed in placebo-treated animals. Progressive improvement after 12 weeks is observed in high-dose-treated animals. (*$P = 0.02$ vs. placebo; †$P = 0.01$ week 12 vs. week 24).

cardiac differentiation. Since the TGF-β is bound to the stem cells, serum detection is reduced. Therefore, the observation of a significant loss of circulating TGF-β may reflect the first step in cardiac differentiation, i.e. the binding of TGF-β to MSC, might be used as an early marker to evaluate efficacy of MSC treatment.

Our study revealed evidence of a dose–response effect to the MSC therapy. First, both high-dose and low-dose MSCs increased regional function in infarct border zone, which is suggestive of MSCs ability to form or mediate the formation of new contractile tissue. Secondly, in terms of remodelling, the placebo group showed continued infarct expansion and functional depression, whereas the low-dose group prevented infarct expansion while the high-dose group actually produced reverse remodelling at structural and functional levels. Importantly, with high but not the low-dose MSCs there was also contractile improvement in the actual infarct zone. A dose–response effect was further validated by a substantial increase in LVEF in the high but not the low-dose group.

An important issue that warrants mention is the use of autologous MSCs in this trial. Mesenchymal stem cells are prototypic cells for use as an allograft given their immunoprivilege. However, it is possible that autologous cells may offer advantages, avoiding late immunologic clearance.[41] Future work is planned to test the relative benefits of allogeneic vs. autologous grafting of MSCs.

Study limitations

As this study was used to obtain regulatory approval to conduct a human study, we were unable to label the injected cells with a marker such as GFP. Thus, the relative contribution of cell engraftment and differentiation to the remarkable degree of structural and functional recovery reported here cannot be definitively ascertained. Other studies are underway in our laboratory using GFP labelled MSCs and will be reported elsewhere. The marked extent of recovery and reverse remodelling that occurred in the high-dose cell group, make a regenerative effect likely. We did not assess the impact of standard post-MI medical regimens in this study, and it is possible that concurrent therapies could influence the magnitude of therapeutic responses in humans. Current

drug therapies could alter the efficacy, and intriguing early work suggests the possibility that it may enhance the effects.[42]

Conclusion

Here we show that porcine MSCs can be safely harvested from BM of animals post-MI, expanded in culture, and injected intra-operatively. Safety in both the acute surgical settings as well as the long-term was outstanding. In addition, detailed phenotyping using cardiac MRI reveals that the cells cause substantial reverse remodelling and restore both tissue perfusion as well as regional contractile restoration in infarct border zones, leading to a net reduction in infarct size and increase in EF. Autologous MSC cell therapy is currently in clinical trials for patients with ischaemic cardiomyopathy.

Acknowledgements

The authors thank Melissa Jones and Jeff Brawn for excellent technical assistance performing the animal surgery and providing outstanding post-operative animal care. The authors also thank Norman J. Barker for his expertise in histological imaging.

Funding

This work was supported by National Heart, Lung, and Blood Institute grants U54-HL081028 (Specialized Center for Cell Based Therapy) and R01-HL084275. J.M.H. is also supported by RO1's AG025017, HL065455, and HL094849. E.S.W. is the Irene Piccinini Investigator in Cardiac Surgery and receives support from the Ruth L. Kirschstein National Research Service Award (NIH 2T32DK007713-12).

Conflict of interest: none declared.

References

1. Mosterd A, Hoes AW. Clinical epidemiology of heart failure. *Heart* 2007;**93**:1137–1146.
2. Ntusi NB, Mayosi BM. Epidemiology of heart failure in sub-Saharan Africa. *Expert Rev Cardiovasc Ther* 2009;**7**:169–180.
3. Lloyd-Jones D, Adams R, Carnethon M, De SG, Ferguson TB, Flegal K, Ford E, Furie K, Go A, Greenlund K, Haase N, Hailpern S, Ho M, Howard V, Kissela B, Kittner S, Lackland D, Lisabeth L, Marelli A, McDermott M, Meigs J, Mozaffarian D, Nichol G, O'Donnell C, Roger V, Rosamond W, Sacco R, Sorlie P, Stafford R, Steinberger J, Thom T, Wasserthiel-Smoller S, Wong N, Wylie-Rosett J, Hong Y. Heart disease and stroke statistics–2009 update: a report from the American Heart Association Statistics Committee and Stroke Statistics Subcommittee. *Circulation* 2009;**119**:480–486.
4. Boyle AJ, Schulman SP, Hare JM, Oettgen P. Is stem cell therapy ready for patients? Stem cell therapy for cardiac repair. ready for the next step. *Circulation* 2006;**114**:339–352.
5. Pittenger MF, Mackay AM, Beck SC, Jaiswal RK, Douglas R, Mosca JD, Moorman MA, Simonetti DW, Craig S, Marshak DR. Multilineage potential of adult human mesenchymal stem cells. *Science* 1999;**284**:143–147.
6. Schuleri KH, Boyle AJ, Hare JM. Mesenchymal stem cells for cardiac regenerative therapy. *Handb Exp Pharmacol* 2007;195–218.
7. Porada CD, Zanjani ED, meida-Porad G. Adult mesenchymal stem cells: a pluripotent population with multiple applications. *Curr Stem Cell Res Ther* 2006;**1**:365–369.
8. Amado LC, Saliaris AP, Schuleri KH, St John M, Xie JS, Cattaneo S, Durand DJ, Fitton T, Kuang JQ, Stewart G, Lehrke S, Baumgartner WW, Martin BJ, Heldman AW, Hare JM. Cardiac repair with intramyocardial injection of allogeneic mesenchymal stem cells after myocardial infarction. *Proc Natl Acad Sci USA* 2005;**102**:11474–11479.
9. Amado LC, Schuleri KH, Saliaris AP, Boyle AJ, Helm R, Oskouei B, Centola M, Eneboe V, Young R, Lima JA, Lardo AC, Heldman AW, Hare JM. Multimodality noninvasive imaging demonstrates in vivo cardiac regeneration after mesenchymal stem cell therapy. *J Am Coll Cardiol* 2006;**48**:2116–2124.
10. Silva GV, Litovsky S, Assad JA, Sousa AL, Martin BJ, Vela D, Coulter SC, Lin J, Ober J, Vaughn WK, Branco RV, Oliveira EM, He R, Geng YJ, Willerson JT, Perin EC. Mesenchymal stem cells differentiate into an endothelial phenotype, enhance vascular density, and improve heart function in a canine chronic ischemia model. *Circulation* 2005;**111**:150–156.
11. Schuleri KH, Amado LC, Boyle AJ, Centola M, Saliaris AP, Gutman MR, Hatzistergos KE, Oskouei BN, Zimmet JM, Young RG, Heldman AW, Lardo AC, Hare JM. Early improvement in cardiac tissue perfusion due to mesenchymal stem cells. *Am J Physiol Heart Circ Physiol* 2008;**294**:H2002–H2011.
12. Chen SL, Fang WW, Ye F, Liu YH, Qian J, Shan SJ, Zhang JJ, Chunhua RZ, Liao LM, Lin S, Sun JP. Effect on left ventricular function of intracoronary transplantation of autologous bone marrow mesenchymal stem cell in patients with acute myocardial infarction. *Am J Cardiol* 2004;**94**:92–95.
13. Katritsis DG, Sotiropoulou PA, Karvouni E, Karabinos I, Korovesis S, Perez SA, Voridis EM, Papamichail M. Transcoronary transplantation of autologous mesenchymal stem cells and endothelial progenitors into infarcted human myocardium. *Catheter Cardiovasc Interv* 2005;**65**:321–329.
14. Bonab MM, Alimoghaddam K, Talebian F, Ghaffari SH, Ghavamzadeh A, Nikbin B. Aging of mesenchymal stem cell in vitro. *BMC Cell Biol* 2006;**7**:14.
15. Aguilar S, Nye E, Chan J, Loebinger M, Spencer-Dene B, Fisk N, Stamp G, Bonnet D, Janes SM. Murine but not human mesenchymal stem cells generate osteosarcoma-like lesions in the lung. *Stem Cells* 2007;**25**:1586–1594.
16. Tolar J, Nauta AJ, Osborn MJ, Panoskaltsis MA, McElmurry RT, Bell S, Xia L, Zhou N, Riddle M, Schroeder TM, Westendorf JJ, McIvor RS, Hogendoorn PC, Szuhai K, Oseth L, Hirsch B, Yant SR, Kay MA, Peister A, Prockop DJ, Fibbe WE, Blazar BR. Sarcoma derived from cultured mesenchymal stem cells. *Stem Cells* 2007;**25**:371–379.
17. Breitbach M, Bostani T, Roell W, Xia Y, Dewald O, Nygren JM, Fries JW, Tiemann K, Bohlen H, Hescheler J, Welz A, Bloch W, Jacobsen SE, Fleischmann BK. Potential risks of bone marrow cell transplantation into infarcted hearts. *Blood* 2007;**110**:1362–1369.
18. Mishra PJ, Mishra PJ, Humeniuk R, Medina DJ, Alexe G, Mesirov JP, Ganesan S, Glod JW, Banerjee D. Carcinoma-associated fibroblast-like differentiation of human mesenchymal stem cells. *Cancer Res* 2008;**68**:4331–4339.
19. Schuleri KH, Boyle AJ, Centola M, Amado LC, Evers R, Zimmet JM, Evers KS, Ostbye KM, Scorpio DG, Hare JM, Lardo AC. The adult Gottingen minipig as a model for chronic heart failure after myocardial infarction: focus on cardiovascular imaging and regenerative therapies. *Comp Med* 2008;**58**:568–579.
20. Wang Y, Huso DL, Harrington J, Kellner J, Jeong DK, Turney J, McNiece IK. Outgrowth of a transformed cell population derived from normal human BM mesenchymal stem cell culture. *Cytotherapy* 2005;**7**:509–519.
21. Slavin GS, Saranathan M. FIESTA-ET: high-resolution cardiac imaging using echo-planar steady-state free precession. *Magn Reson Med* 2002;**48**:934–941.
22. Simonetti OP, Kim RJ, Fieno DS, Hillenbrand HB, Wu E, Bundy JM, Finn JP, Judd RM. An improved MR imaging technique for the visualization of myocardial infarction. *Radiology* 2001;**218**:215–223.
23. Klocke FJ, Simonetti OP, Judd RM, Kim RJ, Harris KR, Hedjbeli S, Fieno DS, Miller S, Chen V, Parker MA. Limits of detection of regional differences in vasodilated flow in viable myocardium by first-pass magnetic resonance perfusion imaging. *Circulation* 2001;**104**:2412–2416.
24. Heiberg E, Engblom H, Engvall J, Hedstrom E, Ugander M, Arheden H. Semi-automatic quantification of myocardial infarction from delayed contrast enhanced magnetic resonance imaging. *Scand Cardiovasc J* 2005;**39**:267–275.
25. Nagaya N, Kangawa K, Itoh T, Iwase T, Murakami S, Miyahara Y, Fujii T, Uematsu M, Ohgushi H, Yamagishi M, Tokudome T, Mori H, Miyatake K, Kitamura S. Transplantation of mesenchymal stem cells improves cardiac function in a rat model of dilated cardiomyopathy. *Circulation* 2005;**112**:1128–1135.
26. Roberts WC, Kaufman RJ. Calcification of healed myocardial infarcts. *Am J Cardiol* 1987;**60**:28–32.
27. Ribeiro KC, Mattos EC, Werneck-de-castro JP, Ribeiro VP, Costa-e-Sousa RH, Miranda A, Olivares EL, Farina M, Mill JG, Goldenberg JR, Masuda MO, de Carvalho AC. Ectopic ossification in the scar tissue of rats with myocardial infarction. *Cell Transplant* 2006;**15**:389–397.
28. Hagege AA, Marolleau JP, Vilquin JT, Alheritiere A, Peyrard S, Duboc D, Abergel E, Messas E, Mousseaux E, Schwartz K, Desnos M, Menasche P. Skeletal myoblast transplantation in ischemic heart failure: long-term follow-up of the first phase I cohort of patients. *Circulation* 2006;**114**:I108–I113.
29. Menasche P, Alfieri O, Janssens S, McKenna W, Reichenspurner H, Trinquart L, Vilquin JT, Marolleau JP, Seymour B, Larghero J, Lake S, Chatellier G, Solomon S, Desnos M, Hagege AA. The Myoblast Autologous Grafting in Ischemic Cardiomyopathy (MAGIC) trial: first randomized placebo-controlled study of myoblast transplantation. *Circulation* 2008;**117**:1189–1200.
30. Ma J, Ge J, Zhang S, Sun A, Shen J, Chen L, Wang K, Zou Y. Time course of myocardial stromal cell-derived factor 1 expression and beneficial effects of

intravenously administered bone marrow stem cells in rats with experimental myocardial infarction. *Basic Res Cardiol* 2005;**100**:217–223.
31. Abbott JD, Huang Y, Liu D, Hickey R, Krause DS, Giordano FJ. Stromal cell-derived factor-1alpha plays a critical role in stem cell recruitment to the heart after myocardial infarction but is not sufficient to induce homing in the absence of injury. *Circulation* 2004;**110**:3300–3305.
32. Kinnaird T, Stabile E, Burnett MS, Shou M, Lee CW, Barr S, Fuchs S, Epstein SE. Local delivery of marrow-derived stromal cells augments collateral perfusion through paracrine mechanisms. *Circulation* 2004;**109**:1543–1549.
33. Gnecchi M, He H, Liang OD, Melo LG, Morello F, Mu H, Noiseux N, Zhang L, Pratt RE, Ingwall JS, Dzau VJ. Paracrine action accounts for marked protection of ischemic heart by Akt-modified mesenchymal stem cells. *Nat Med* 2005;**11**: 367–368.
34. Mazhari R, Hare JM. Mechanisms of action of mesenchymal stem cells in cardiac repair: potential influences on the cardiac stem cell niche. *Nat Clin Pract Cardiovasc Med* 2007;**4**(Suppl. 1):S21–S26.
35. Ohnishi S, Sumiyoshi H, Kitamura S, Nagaya N. Mesenchymal stem cells attenuate cardiac fibroblast proliferation and collagen synthesis through paracrine actions. *FEBS Lett* 2007;**581**:3961–3966.
36. Behfar A, Zingman LV, Hodgson DM, Rauzier JM, Kane GC, Terzic A, Puceat M. Stem cell differentiation requires a paracrine pathway in the heart. *FASEB J* 2002; **16**:1558–1566.
37. Kofidis T, de Bruin JL, Yamane T, Tanaka M, Lebl DR, Swijnenburg RJ, Weissman IL, Robbins RC. Stimulation of paracrine pathways with growth factors enhances embryonic stem cell engraftment and host-specific differentiation in the heart after ischemic myocardial injury. *Circulation* 2005;**111**: 2486–2493.
38. Sachinidis A, Kolossov E, Fleischmann BK, Hescheler J. Generation of cardiomyocytes from embryonic stem cells experimental studies. *Herz* 2002;**27**: 589–597.
39. Chang SA, Lee EJ, Kang HJ, Zhang SY, Kim JH, Li L, Youn SW, Lee CS, Kim KH, Won JY, Sohn JW, Park KW, Cho HJ, Yang SE, Oh WI, Yang YS, Ho WK, Park YB, Kim HS. Impact of myocardial infarct proteins and oscillating pressure on the differentiation of mesenchymal stem cells: effect of acute myocardial infarction on stem cell differentiation. *Stem Cells* 2008;**26**:1901–1912.
40. Aggarwal S, Pittenger MF. Human mesenchymal stem cells modulate allogeneic immune cell responses. *Blood* 2005;**105**:1815–1822.
41. Hare JM, Chaparro SV. Cardiac regeneration and stem cell therapy. *Curr Opin Organ Transplant* 2008;**13**:536–542.
42. Boyle AJ, Schuster M, Witkowski P, Xiang G, Seki T, Way K, Itescu S. Additive effects of endothelial progenitor cells combined with ACE inhibition and beta-blockade on left ventricular function following acute myocardial infarction. *J Renin Angiotensin Aldosterone Syst* 2005;**6**:33–37.